# DESIGN OF ONE DEGREE OF FREEDOM CLOSED LOOP SPATIAL CHAINS USING NON-CIRCULAR GEARS

By

MANDAR SHRIKANT HARSHE

A THESIS PRESENTED TO THE GRADUATE SCHOOL
OF THE UNIVERSITY OF FLORIDA IN PARTIAL FULFILLMENT
OF THE REQUIREMENTS FOR THE DEGREE OF
MASTER OF SCIENCE

UNIVERSITY OF FLORIDA

2009

I have to understand the world, you see.

- Richard Feynman, Physicist (1918 - 1988)

ACKNOWLEDGMENTS

I am extremely grateful to my supervisory committee chair, Dr. Carl D. Crane III, for giving me an opportunity to work at CIMAR. His guidance and support throughout the duration of my study made this work possible and gave direction to my work. I also thank Dr. David Dooner, of University of Puerto Rico - Mayagüez, with whom we collaborated on this project. His guidance and support helped me immensely in this work. I would like to thank Dr. John Schueller and Dr. A. Antonio Arroyo for agreeing to be on my committee.

I would like to acknowledge the support provided by the Department of Energy via the University Research Program in Robotics (URPR) through University of Florida grant number DE-FG04-86NE37967.

I received great support from my friends and colleagues, including Vishesh Vikas, Sanketh Bhat and Priyank Bagrecha. I am extremely grateful for their words of encouragement and support. I also thank fellow students at CIMAR. Finally, I am indebted to my parents and my sister for their love and support; I owe my success and progress to them.

TABLE OF CONTENTS

LIST OF TABLES

LIST OF FIGURES

Abstract of Thesis Presented to the Graduate School
of the University of Florida in Partial Fulfillment of the
Requirements for the Degree of Master of Science

DESIGN OF ONE DEGREE OF FREEDOM CLOSED LOOP SPATIAL CHAINS
USING NON-CIRCULAR GEARS

By

Mandar Shrikant Harshe

May 2009

Chair: Carl D. Crane III
Major: Mechanical Engineering

Real world robot manipulators often use open-loop geometry where the motions governing positioning are independent from those controlling the orientation of the objects. These types of robot manipulators need expensive hardware and complicated controllers to manipulate the multiple (generally six) actuators. This research presents the design of one degree-of-freedom spatial mechanisms that use non-circular gears to constrain the motion. The geometry of one degree-of-freedom mechanisms and the design of the non-circular gears that link certain joint axes has already been dealt with. This research is concerned with the design of mechanism parameters like link lengths, joint offsets, and twist angles when the gear profiles are known.

In a spatial body-guidance problem, representing the motion by systems of polynomial equations restricts the number of end-effector positions and orientations (end-effector poses) that can be used as inputs for mechanism design. An approach has been developed that takes any number of desired poses as guide points and develops a mechanism that approximately attains the desired poses over the course of its motion. A problem with implementing this design strategy is the inherent difficulty in accounting for orientation and position errors. The approach described here addresses this problem by defining a new error functional, calculated in the joint space domain. As the mechanisms being dealt with are single degree-of-freedom closed chains, the starting position is a crucial decision in the design process. The method outlines the choice of the starting position and details how

this error term can be used along with optimization techniques on either the mechanism parameters or the non-circular gears. Numerical examples are presented.

# CHAPTER 1
# INTRODUCTION

## 1.1 Motivation

The most common use of robot manipulators is in industrial environments where the focus is on repetitive motions. In such cases, the manipulator has only one set of motions and uses multiple actuators to achieve it. Essentially, a multiple degree-of-freedom device is utilized to perform a fixed set of actions. These fixed actions can be represented in terms of a single parameter. For these kinds of repetitive tasks we can consider developing single degree-of-freedom spatial manipulators. This new class of mechanisms can be designed such that the end-effector traces out the desired path, manipulating the object's position and orientation.

To design this new class of mechanisms, we can either employ exact synthesis or accurate synthesis. In exact synthesis, we design the mechanism to guide the rigid body or end-effector exactly through the precision points while in accurate synthesis the mechanism designed is such that it optimizes a certain objective function that depends upon the precision points. The design specifications are the set of end effector positions and orientations to be attained in a given order. The design parameters are the mechanism parameters, such as link lengths, joint offsets and twist angles, and the location of the bases with respect to the desired poses. A listing of such methods that deal with geometric design has been presented by (1).

Methods involving exact synthesis require that the number of independent design equations must be less than or equal to the number of design parameters. This puts a limit on the number of precision points that can be defined on a path (2–4). The complexity of the problem increases as the number of precision points increase and methods like interval analysis (5) or polynomial continuation (6–9) are used to solve the equations generated. Approximate synthesis allows us to use more precision points, with

optimization techniques being used to design the mechanism parameters. This necessitates a valid objective function to be defined.

In the case of planar mechanism design, methods like approximate synthesis and accurate synthesis are used. These methods use the position of a point on the coupler link as the output function and define the objective function as the difference between the desired and actual positions. (10) shows a method for designing three dimensional links that also uses only the position of the coupler point to design the four bar linkage. Others, (11; 12) use the condition number as an objective function to design spatial manipulators.

In this research the focus is on defining an error functional that can be used as an objective function for optimization techniques. This error functional should include the errors between the desired and actual position and orientations of the end-effector. The most common way of doing this is to first calculate the position error. To calculate the orientation error, the angular differences in the corresponding x,y,z axes of the desired and actual coordinate systems attached to the end-effectors are converted to length scales. The choice of this multiplication factor is subjective and essentially decides which of the position or orientation error must be given priority. This problem is addressed by defining the error in the joint angle domain space.

## 1.2 Related work

This work is focused extensively on a class of closed loop serial chains that possess a special geometry. In order to incorporate gears between specific links, pairs of adjacent joint axes were set to be parallel. An example which demonstrates this geometry is shown in Figure 1-1. The work done in (13) focused on the same geometry and demonstrated a solution to the inverse position analysis of each of the two subchains. For the given geometry, it was proved that up to 16 real solutions exist for each subchain for a given pose. Further work was done and (14) dealt with designing non-circular gears for the given mechanism, that would allow the end-effector to accurately reach each pose. However it is difficult to ensure that the gear profile remains feasible. In almost all cases, the calculated

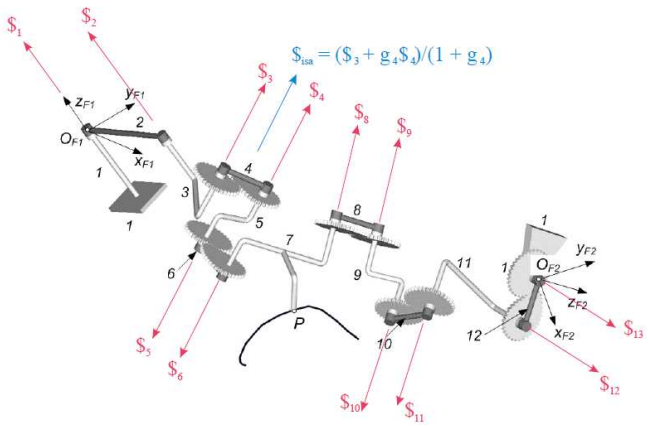


Figure 1-1. A 12-link, 1-degree of freedom manipulator

gear ratios varied from positive values to negative values. This implied that for certain sections of the path, internal gears were necessary while for other sections external gears would be needed. Implementing such solutions is practically not feasible.

Another way of looking at the problem is to treat the gear ratios as fixed, and develop a scheme that designs the mechanism parameters so that rigid body guidance is possible. This type of design is dealt in (15), where a design strategy using optimization for open loop chains is explained. A similar method is employed in (16) where Fourier Analysis is used to aid the design synthesis. However, in both these approaches, the focus is on force or energy related design criteria. The optimization approach was used to develop an open loop chain such that the end-effector best approximates the desired set of poses. For the purpose of optimization, the paper describes a method that uses the orientation to parameterize the curves and define a correspondence point that can be used to calculate the error. The Fourier Analysis approach aims to perform number and dimensional synthesis.

In this research, the geometry of the mechanism is already known. The dimensional synthesis is the aim of the design. Also, a purely kinematic approach is taken and any energy or force considerations are ignored in the design. The path is parameterized in terms of the input angle but a completely different error functional is developed. The

geometry of the chain gives rise to multiple solutions, and a method must be developed to systematically deal with these and choose the "best" solution. This kind of scenario does not arise in other geometries. This method addresses this problem and also attempts to define an error functional that does not include non-homogeneous terms. The error measure is also well-defined in the sense that the term calculated has physical significance.

# CHAPTER 2
# PROBLEM STATEMENT AND APPROACH

The mechanism to be designed has the geometry as shown in Fig. 2-1. The pairs of axes that are parallel to each other are $(\$_1, \$_2)$, $(\$_3, \$_4)$, $(\$_5, \$_6)$, $(\$_7, \$_8)$, $(\$_9, \$_{10})$ and $(\$_{11}, \$_{12})$, where $\$_i$ refers to the joint between links $i$ and $i+1$. For this type of geometry, the mechanism parameters are given by the condition:

$$\begin{aligned} \alpha_{12},\ \alpha_{34},\ \alpha_{56} &= 0 \\ \alpha_{78},\ \alpha_{9,10},\ \alpha_{11,12} &= 0 \end{aligned} \tag{2–1}$$

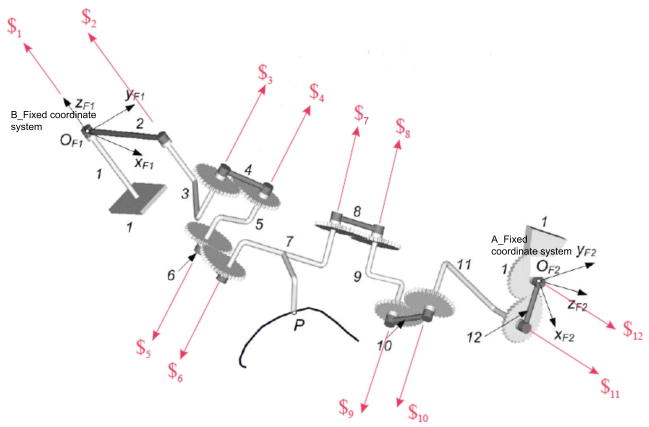


Figure 2-1. A candidate mechanism

The mechanism can be treated as two 6 link open chains with coincident end-effectors. The side containing 3 gear pairs is called the A side and the side containing 2 gear pairs is called the B side. Coordinate systems are attached to the base of the A and B side and also at the end-effector. The *'A_ fixed'*coordinate system has the origin on $\$_{12}$). The *'B_ fixed'* coordinate system has the origin fixed on $\$_1$ with the z axis along $\$_1/$. The *'tool'* coordinate system is fixed to the end-effector and represents the location and orientation of the end-effector. The parameters needed for designing the mechanism are:

${}^{B\_fixed}_{A\_fixed}\mathbf{T}$**:** Pose of *'A_ fixed'* coordinate system with respect to *'B_ fixed'* coordinate system

${}^{6B}_{tool}\mathbf{T}$**:** Pose of *'tool'* coordinate system with respect to *'6B'* coordinate system

${}^{6B}_{6A}\mathbf{T}$: Pose of *'6A'* coordinate system with respect to *'6B'* coordinate system

${}^{B\_fixed}_{tool}\mathbf{T}$: Required poses of the tool coordinate system measured with respect to the *'B_fixed'* coordinate system

A candidate design is evaluated by sweeping the input angle of a candidate mechanism to reach the given desired poses. $P_i$ is the $4 \times 4$ matrix that defines the desired position and orientation of the end effector at the $i^{th}$ pose. A reverse analysis as outlined by (13) is performed which results in up to 16 real solutions for each pose. We note that each of the real solutions is valid and could be achieved.

Since this is a rigid body guidance problem, the path is defined by a set of matrices $P_i$ which must be reached in a particular order. In order to effectively use approximate synthesis with optimization, the path must be described using a parametric representation. This parameter will also allow us to define corresponding points on similar paths. The gears coupling the parallel joint axes result in the mechanism being a single degree-of-freedom serial chain and hence, the path traced out by the end-effector can be represented in terms of one parameter. The input angle $\phi$ (the first angle on the B side) is used as this parameter. The focus here is to describe the motion in terms of joint angles as opposed to in terms of the path coordinates.

If the starting configuration of the candidate mechanism is known, the input angle can be effectively used to describe the motion of the end-effector, for that starting configuration. This can be achieved by using a screw theory approach (17; 18) and iteratively using the velocity equations to find the position of the end-effector corresponding to each value of the input angle. It is thus noted that each solution in the set of joint angles $\grave{\mathrm{U}}_1^j$ will give rise to a different behavior of the end-effector, and also a different path.

Thus, we end up with the desired path and sets of actual paths all represented in terms of the starting configuration and parameterized in terms of the input joint angle. Points on different paths that are represented by the same value of input angle are defined to be correspondence points. The error is then defined in terms of the difference in the

joint angles obtained to make the end-effector reach the actual pose, and those obtained as the mechanism traces out its path. The joint angles on the B side are used to calculate this error. Weighting factors are used since the contribution of each joint is not the same. Each generated path thus gives us an error value and we can then select the best starting configuration. This gives an error measure for the mechanism, which can be used as the optimization objective function. This procedure is detailed in the next chapter.

# CHAPTER 3
# DESIGN METHOD

## 3.1 Actual Path Generation

In order to analyze the motion of the mechanism, it is treated as two 6 link open chains with coincident end-effectors. The side containing 3 gear pairs is called the A side and the side containing 2 gear pairs is called the B side. The motion of the mechanism is represented by the set of joint angles of the A and B sides as the input angle changes from one value to another value. To calculate these, the screw theory based approach is used incrementally. A small step size is chosen and the Plucker coordinates of the joint axes for the current set of joint angles are determined using methods detailed by (13; 19; 20). Considering the end-effector as a part of the A (or B) side of the mechanism, the velocity of the end-effector is given by Eqn. (3–1) (21).

$$ {}_0\omega_1 \cdot_0 \$_1 +_1 \omega_2 \cdot_1 \$_2 +_2 \omega_3 \cdot_2 \$_3 +_3 \omega_4 \cdot_0 \$_4 +_4 \omega_5 \cdot_4 \$_5 +_5 \omega_6 \cdot_5 \$_6 = \omega_7 \cdot \$_7 \tag{3–1} $$

Here, ${}_{i-1}\omega_i$ represents the angular velocity of link $i+1$ with respect to link $i$. ${}_{i-1}\$_i$ represents the screw (or the Plucker coordinates) about which link $i+1$ moves, with respect to link $i$. Since all joints are assumed revolute here, ${}_{i-1}\$_i$ represent the joint axes. $\$_7$ represents the screw about which the end-effector moves with respect to ground and $\omega_7$ is the corresponding angular velocity.

However, due to the presence of gears, the equations simplify greatly. For the A side, the three gear pairs reduce the equation to one in the three unknown angular velocities, as given in Eqn. (3–2). The B side reduces to Eqn. (3–3) in 4 angular velocities, of which one is the known input angular velocity (${}_0\omega_1$) of the first joint.

$$ {}_0\omega_1^A \cdot ({}_0\$_1^A +_1 g_2^A \cdot_1 \$_2^A) +_2 \omega_3 \cdot ({}_2\$_3^A +_3 g_4^A \cdot_3 \$_4^A) +_4 \omega_5 \cdot ({}_4\$_5^A +_5 g_6^A \cdot_5 \$_6^A) = \omega_7 \cdot \$_7 \tag{3–2} $$

$$ {}_0\omega_1^B \cdot_0 \$_1^B +_1 \omega_2^B \cdot ({}_1\$_2^B +_2 g_3^B \cdot_2 \$_3^B) +_3 \omega_4^B \cdot ({}_3\$_4^B +_4 g_5^B \cdot_4 \$_5^B) +_5 \omega_6^B \cdot_5 \$_6^B = \omega_7 \cdot \$_7 \tag{3–3} $$

Equation 3–2 and Eqn. 3–3 gives Eqn. 3–4 which represent 6 scalar equations in 6 unknown angular velocities. These equations are then solved and the B side joint angles are updated for a small change of the input angle, by using Eqns. 3–5. A forward analysis of the B side is done to get the updated end effector pose and this is then used to get the exact joint angles for the A side by inverse analysis. As inverse analysis give rise to multiple solutions, the new angles that are closest to the previous set of angles are chosen.

$$\begin{aligned} {}_0\omega_1^A \cdot ({}_0\$_1^A +_1 g_2^A \cdot_1 \$_2^A) +_2 \omega_3 \cdot ({}_2\$_3^A +_3 g_4^A \cdot_3 \$_4^A) +_4 \omega_5 \cdot ({}_4\$_5^A +_5 g_6^A \cdot_5 \$_6^A) = \\ {}_0\omega_1^B \cdot_0 \$_1^B +_1 \omega_2^B \cdot ({}_1\$_2^B +_2 g3^B \cdot_2 \$_3^B) +_3 \omega_4^B \cdot ({}_3\$_4^B +_2 g3_4^B\$_5^B) +_5 \omega_6^B \cdot_5 \$_6^B \end{aligned} \tag{3–4}$$

$$\begin{aligned} ({}_0\varphi_{1B})_{i+1} &= ({}_0\varphi_{1B})_i + \Delta\varphi \\ ({}_1\theta_{2B})_{i+1} &= ({}_1\theta_{2B})_i + (\frac{{}^1\omega_2}{{}_0\omega_1})\Delta\varphi \\ ({}_2\theta_{3B})_{i+1} &= ({}_2\theta_{3B})_i + (\frac{{}^2\omega_3}{{}_0\omega_1})\Delta\varphi \\ ({}_3\theta_{4B})_{i+1} &= ({}_3\theta_{4B})_i + (\frac{{}^3\omega_4}{{}_0\omega_1})\Delta\varphi \\ ({}_4\theta_{5B})_{i+1} &= ({}_4\theta_{5B})_i + (\frac{{}^4\omega_5}{{}_0\omega_1})\Delta\varphi \\ ({}_5\theta_{6B})_{i+1} &= ({}_5\theta_{6B})_i + (\frac{{}^5\omega_6}{{}_0\omega_1})\Delta\varphi \end{aligned} \tag{3–5}$$

A case study for this method shows us that this method indeed gives the correct motion for the closed loop chain as the input angle is swept. This was done by performing the calculations as given by Equations 3–5 to get new angles. Then using these new angles, the displacement analyses of the A and B side are performed to get all the screw axes coordinates. This iterative method using Equations 3–4 and 3–5, gives us the joint angles for the entire range of motion. The mechanism parameters chosen for this case study are given in Table 3-1 and Table 3-2 with the other parameters given in Table 3-3.

Figure 3-1 and Fig. 3-2 show the variation of the angles as the input angle sweeps from its initial value by 0.5 radians. The gears were all chosen to have 1:1 ratios. Figure 3-3 shows that all calculated gear ratios (by forward difference method) closely approximate the actual ratios of 1. A smaller value of step size $\Delta\varphi$ gives values closer to

Table 3-1. Mechanism parameters for A side

| Offset distance (in.) | Linklengths (in.) | Twist angles (deg) |
|---|---|---|
| $S_2 = 6$ | $a_{12} = 3$ | $\alpha_{12} = 0$ |
| $S_3 = 0$ | $a_{23} = 10$ | $\alpha_{23} = 90$ |
| $S_4 = 6$ | $a_{34} = 3$ | $\alpha_{34} = 0$ |
| $S_5 = 0$ | $a_{45} = 10$ | $\alpha_{45} = 90$ |
| $S_6 = 6$ | $a_{56} = 3$ | $\alpha_{56} = 0$ |

Table 3-2. Mechanism parameters for B side

| Offset distance (in.) | Linklengths (in.) | Twist angles (deg) |
|---|---|---|
| $S_2 = 6$ | $a_{12} = 4$ | $\alpha_{12} = 0$ |
| $S_3 = 0$ | $a_{23} = 14$ | $\alpha_{23} = 90$ |
| $S_4 = 6$ | $a_{34} = 4$ | $\alpha_{34} = 0$ |
| $S_5 = 0$ | $a_{45} = 12$ | $\alpha_{45} = 90$ |
| $S_6 = 6$ | $a_{56} = 4$ | $\alpha_{56} = 0$ |

1. In Fig. 3-3, the values A12, A34 and A56 denote the three gear ratios for the gear pairs on the A side. A12 is the gear ratio between joints 1 and 2, A34 between joints 3 and 4, and A56 between the joints 5 and 6. As seen from the figure, the calculated values of gear ratios are within 99.5% of the actual values. This is a very good estimate and thus ensures that the method gives a motion that is accurate to a great extent.

### 3.2 Error Measure

The first problem addressed was that of defining an error measure, if the actual path traced by the end-effector of the candidate mechanism was given. Since the input angle is used as a parameter to define the path, the error is defined in the joint angle space

Table 3-3. System parameters

| | |
|---|---|
| ${}^{B\_fixed}_{A\_fixed}\mathrm{T}$ | $\begin{pmatrix} 1 & 0 & 0 & -18 \\ 0 & 0 & -1 & -5 \\ 0 & 1 & 0 & 12 \\ 0 & 0 & 0 & 1 \end{pmatrix}$ |
| ${}^{6B}_{tool}\mathrm{T}$ | $\begin{pmatrix} 1 & 0 & 0 & 4 \\ 0 & 1 & 0 & -2 \\ 0 & 0 & 1 & 3 \\ 0 & 0 & 0 & 1 \end{pmatrix}$ |
| ${}^{6B}_{6A}\mathrm{T}$ | $\begin{pmatrix} -1 & 0 & 0 & 8 \\ 0 & 0 & -1 & 2 \\ 0 & -1 & 0 & 4 \\ 0 & 0 & 0 & 1 \end{pmatrix}$ |

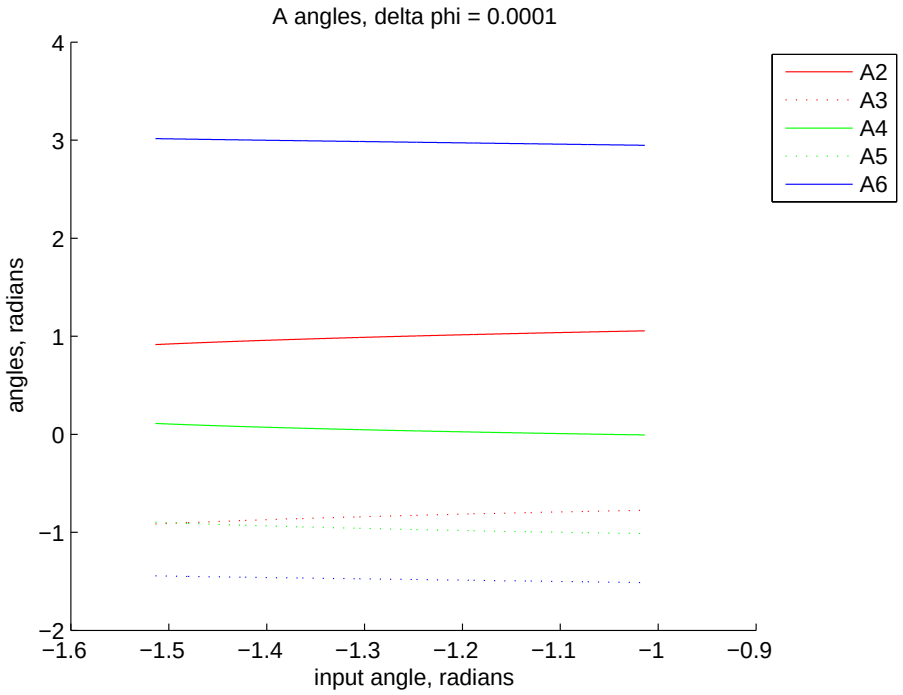


Figure 3-1. Case Study :- A-side angles vs input angle

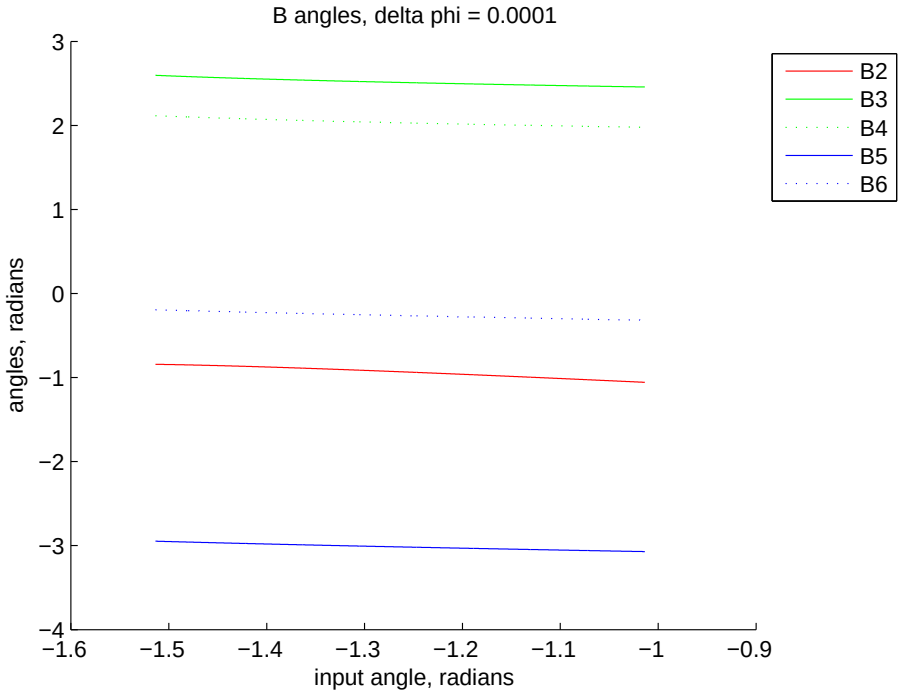


Figure 3-2. Case Study :- B-side angles vs input angle

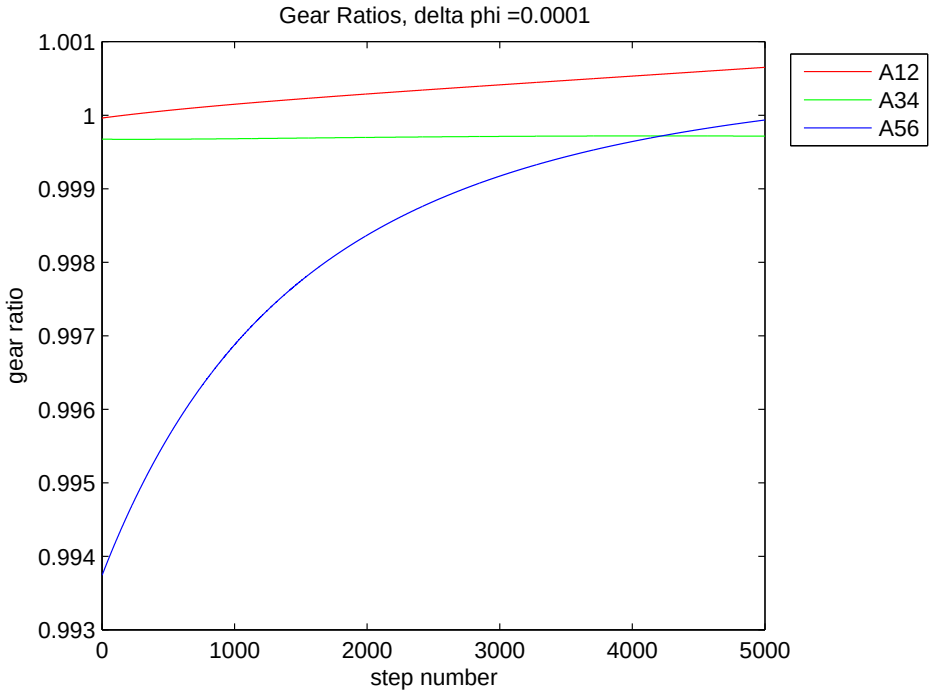


Figure 3-3. Case Study :- Gear ratios (A side) vs step number

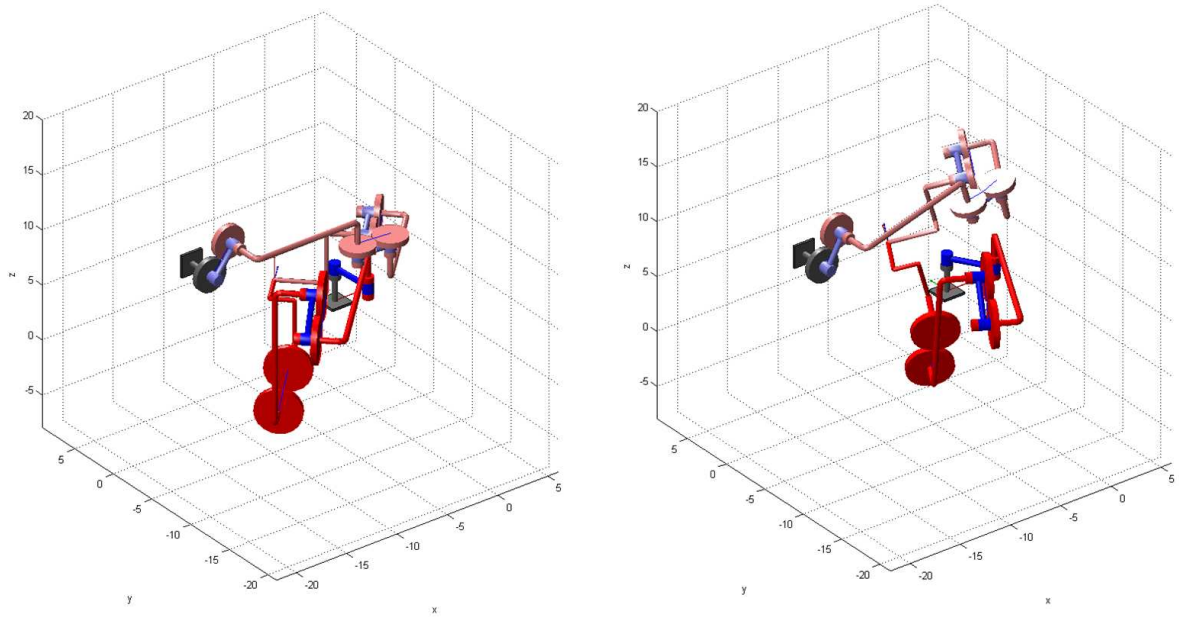

A Start: Configurations 1 for A and B Side

B End: Input angle sweep = 0.5 radians

Figure 3-4. Start and end configurations

domain. The input angle $\phi_i$ required to exactly reach the desired pose $P_{i,desired}$ can be calculated by performing the inverse analysis. The problem of choosing the "correct" solution out of the possible 16 is addressed in the following sections. The actual pose on the path that is said to correspond with this desired pose is that when the input angle $\varphi$ equals the $\phi_i$ which was calculated.

Thus, for pose $P_i$, there exists joint angles $\theta_{ij,desired}$ and $\theta_{ij,actual}$, where j refers to the joint number. For each pose, the error can be defined as:

$$e_i = \left( \sum_{j=2}^{6} (w_i \times |\theta_{ij,desired} - \theta_{ij,actual}|)^2 \right)^{\frac{1}{2}} \tag{3–6}$$

Here, $w_i$ is the weighting factor that is described in the next section. The error for the entire path, can be defined as:

$$E = \sum_i e_i \tag{3–7}$$

### 3.3 Weighting Factor

In calculating the weighting factor, the following observation is made. In a serial chain manipulator, the error in each joint affects the position and orientation of the end-effector. However, this contribution is not uniform. Also, assuming that the joints closer to the base affect the total error more is false. The error in the position of the end-effector due to a certain joint depends on the perpendicular distance of the end effector tool point from the joint axis. As a result, the base joint may not necessarily contribute the largest error. To account for this, a weighting system based on the configuration of the mechanism is defined.

Let $r_0$ be the location of the end-effector in the given configuration. To calculate the weight for *joint i*, the angle $\theta_i$ is varied by a small amount, $\delta\theta$. Let $r_i$ be the new position of the end-effector if the *joint i* is varied by $\delta\theta$. Then, the weight $w_i$ is defined as:

$$w_i = |r_0 - r_i|/\delta\theta \tag{3–8}$$

As the units of the weighting factor are length/angle, the error will have a dimension of length.

### 3.4 Handling Multiple Solutions

The major problem that must be handled is the existence of multiple solutions in the inverse analysis. Each starting configuration will give rise to a different path for the end-effector. The method implemented involves taking each solution into consideration, in order to select the best set of solutions. The score of these best solutions is then evaluated and used as a score for the mechanism.

Let ${}_i\Omega$ be the path generated by the solution $\grave{\mathrm{U}}_1^i$. To evaluate the score for the second pose on this path with respect to the desired second pose, the set of solutions $\hat{\mathrm{U}}_2$ must be chosen from all $\grave{\mathrm{U}}_2^j$, such that the pose corresponding to $\hat{\mathrm{U}}_2$ lies in ${}_i\Omega$.

$\grave{\mathrm{U}}_2^j\{1\}$ is checked for all j. If $\grave{\mathrm{U}}_2^j\{1\} = {}_i\Omega_k\{1\}$ for some $j$ and $k$, the two joint angle sets are said to correspond to the same pose. The ${}_i\Omega_k$ is the joint angle set for the actual pose while the $\grave{\mathrm{U}}_2^j$ represents the desired second pose. The error $e_2^j$ is then calculated for this pose. The same calculations are performed for all $j$, $k$ to get all $e_2^j$. The error for the second pose is then defined as

$$e_2 = \min_j e_2^j \tag{3–9}$$

The error for each pose is calculated using the same method, using Eqn. (3–6) to give $e_l^j$. The error for the pose is then defined as

$$e_l = \min_j e_l^j \tag{3–10}$$

Thus, using Eqn. (3–7), the error for the path ${}_i\Omega$ is given by $E_i$. Since each path ${}_i\Omega$ will give rise to a different error, the best path must be chosen to define the mechanism error. This is done by defining the error E as

$$E = \min_l E_l \tag{3–11}$$

This error E is used as the measure of the mechanism for following the given path and can be used as a optimizing cost function for design.

# CHAPTER 4
# NUMERICAL EXAMPLE

Table 4-1. Mechanism parameters for A side

| Offset distance (in.) | Linklengths (in.) | Twist angles (deg) |
|---|---|---|
| $S_2 = 6$ | $a_{12} = 3$ | $\alpha_{12} = 0$ |
| $S_3 = 0$ | $a_{23} = 10$ | $\alpha_{23} = 90$ |
| $S_4 = 6$ | $a_{34} = 3$ | $\alpha_{34} = 0$ |
| $S_5 = 0$ | $a_{45} = 10$ | $\alpha_{45} = 90$ |
| $S_6 = 6$ | $a_{56} = 3$ | $\alpha_{56} = 0$ |

Table 4-2. Mechanism parameters for B side

| Offset distance (in.) | Linklengths (in.) | Twist angles (deg) |
|---|---|---|
| $S_2 = 3.4947$ | $a_{12} = 14.238$ | $\alpha_{12} = 0$ |
| $S_3 = 0$ | $a_{23} = 0.7411$ | $\alpha_{23} = 59.2992$ |
| $S_4 = 1.3465$ | $a_{34} = 12.9009$ | $\alpha_{34} = 0$ |
| $S_5 = 0$ | $a_{45} = 6.1349$ | $\alpha_{45} = 76.8924$ |
| $S_6 = 6$ | $a_{56} = 10.3782$ | $\alpha_{56} = 0$ |

The results of using this method to generate the error measure of a mechanism on an example set of poses is given below. Table 4-1 and Table 4-2 list the mechanism parameters for the A and the B side respectively. The six desired poses $P_i$ are listed in Table 4-3 and the solutions to reverse analysis for each pose for the A side and B side are calculated. For the given combination of poses and mechanism parameters, the number of solutions obtained for each side is listed in Table 4-4. For this particular example, the all gear pairs are assumed to be circular, with gear ratio 1.

Since there are 2 solutions for A side and 14 for the B side for the starting pose, there are 28 possible starting configurations for the mechanism. The paths taken by the end-effector in each of the 28 cases are shown in Fig. 4-1. At the first pose, the error is zero. Each of these configurations gives us a path that the mechanism end-effector follows. The method described in this paper chooses the solutions given in Table 4-5 for the starting configuration. The input joint angles for the other 5 poses are also listed. Since the mechanism is a one degree-of-freedom serial chain, specifying only the input angles for the successive poses defines the mechanism configuration.

Table 4-3. Desired poses and orientations

| Pose | Transformation matrix (in rad. & in.) |
|---|---|
| Pose 1 | $\begin{pmatrix} -0.4771 & 0.4752 & 0.7393 & 10.1043 \\ -0.5994 & 0.4393 & -0.6691 & -7.9145 \\ -0.6428 & -0.7624 & 0.07524 & 0.6524 \\ 0 & 0 & 0 & 1 \end{pmatrix}$ |
| Pose 2 | $\begin{pmatrix} -0.4498 & 0.4669 & 0.7614 & 9.5769 \\ -0.5949 & 0.4792 & -0.6453 & -8.1136 \\ -0.6662 & -0.7432 & 0.06227 & 0.2199 \\ 0 & 0 & 0 & 1 \end{pmatrix}$ |
| Pose 3 | $\begin{pmatrix} -0.4112 & 0.4773 & 0.7766 & 9.0467 \\ -0.5721 & 0.5281 & -0.6276 & -8.3770 \\ -0.7097 & -0.7023 & 0.0559 & -0.0170 \\ 0 & 0 & 0 & 1 \end{pmatrix}$ |
| Pose 4 | $\begin{pmatrix} -0.3575 & 0.5062 & 0.7848 & 8.5276 \\ -0.5244 & 0.5865 & -0.6172 & -8.8086 \\ -0.7728 & -0.6322 & 0.0558 & -0.1373 \\ 0 & 0 & 0 & 1 \end{pmatrix}$ |
| Pose 5 | $\begin{pmatrix} -0.2803 & 0.5514 & 0.7857 & 8.023 \\ -0.4408 & 0.6531 & -0.6157 & -9.4116 \\ -0.8527 & -0.5190 & 0.0600 & -0.1222 \\ 0 & 0 & 0 & 1 \end{pmatrix}$ |
| Pose 6 | $\begin{pmatrix} -0.1683 & 0.6034 & 0.7795 & 7.5196 \\ -0.3040 & 0.7205 & -0.6233 & -10.1775 \\ -0.9377 & -0.3419 & 0.0621 & -0.0159 \\ 0 & 0 & 0 & 1 \end{pmatrix}$ |

Table 4-4. Number of solutions by reverse analysis

| Pose | A side | B side |
|---|---|---|
| Pose 1 | 2 | 14 |
| Pose 2 | 2 | 14 |
| Pose 3 | 2 | 12 |
| Pose 4 | 2 | 10 |
| Pose 5 | 2 | 8 |
| Pose 6 | 2 | 6 |

Table 4-5. Solutions selected for min. error criteria

| | |
|---|---|
| Starting joint angles, A side | [ 0.5885 −0.5885 0.7094 −1.4948 2.8749 −1.3041 ] |
| Starting joint angles, B side | [ 2.1040 0.0805 3.1074 1.6535 −3.1309 1.7276 ] |
| Pose 2 Input angle | 2.1890 |
| Pose 3 Input angle | 2.2890 |
| Pose 4 Input angle | 2.3890 |
| Pose 5 Input angle | 2.4890 |
| Pose 6 Input angle | 2.5890 |

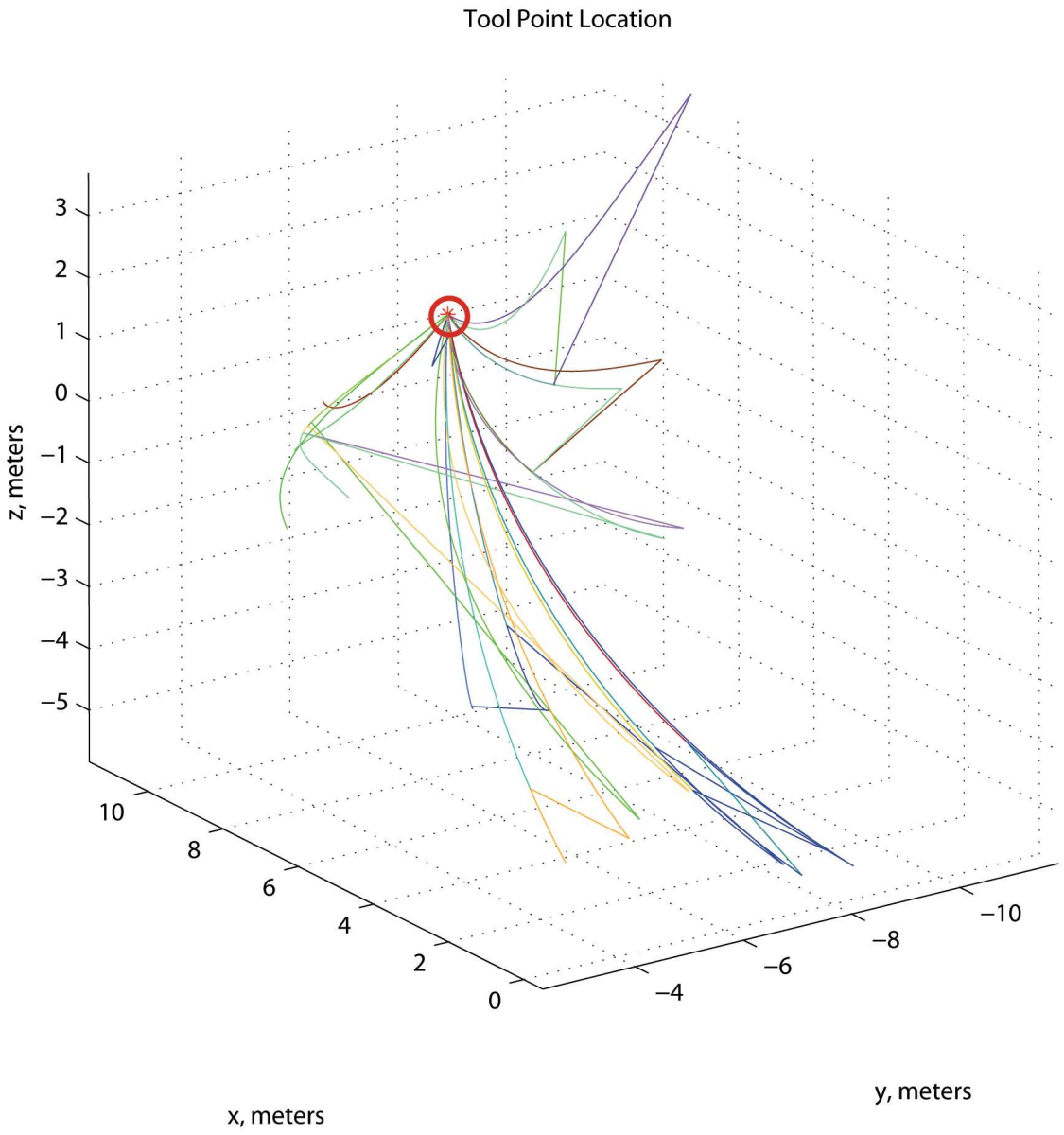


Figure 4-1. The different paths traced by end-effector when different starting configurations are chosen. All paths start from the same starting pose, highlighted in red.

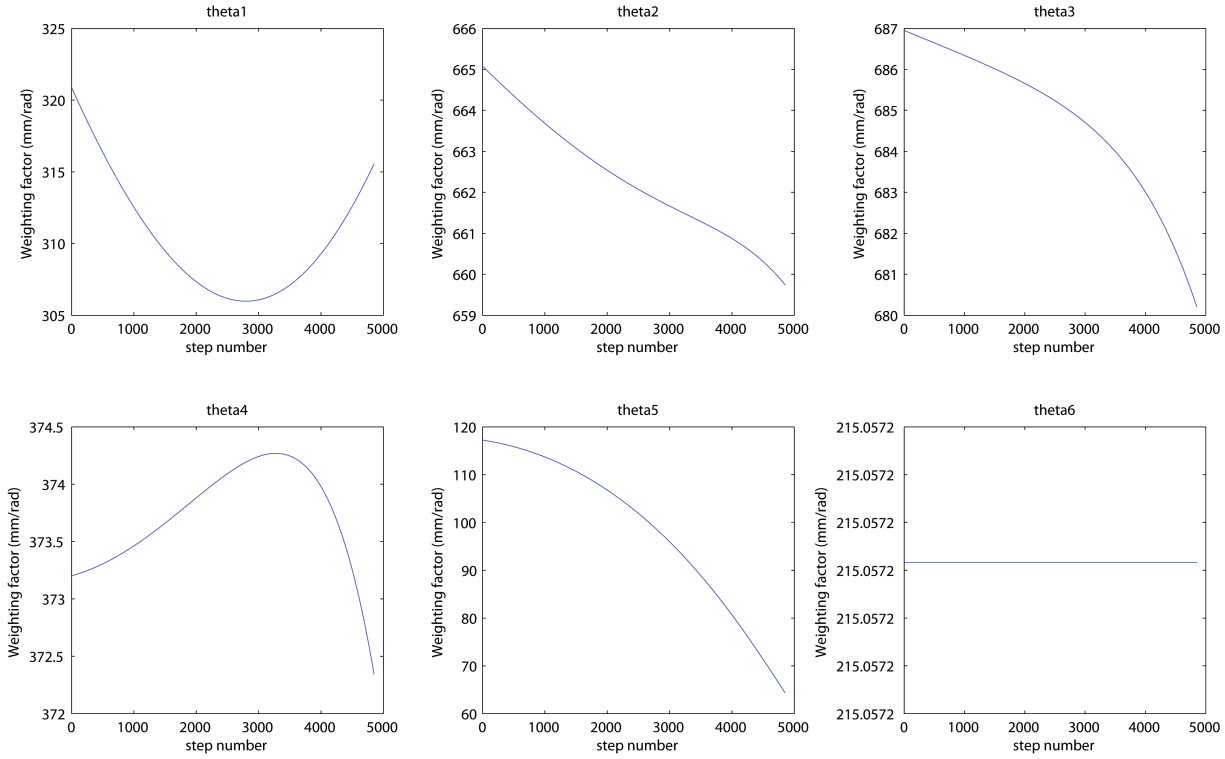


Figure 4-2. Variation of the weighting factors as the mechanism sweeps over the selected "best" path

The variation of the weighting factors for the selected path are shown in Fig. 4-2. While the changes in the weighting factors are not large, they demonstrate the fact that the contribution of the angles depends on the current orientation. As can be seen from the figure, the $\theta_2$ and $\theta_3$ have a greater effect than $\theta_1$ on the end-effector error. For the mechanism presented, the error was calculated to be 42.49 mm.

# CHAPTER 5
# CONCLUSIONS

A method for the design of one degree of freedom, closed loop spatial chains that utilize planar non-circular gears was presented in this thesis. The method addressed an important problem of accounting for orientation errors along with position errors in the rigid body guidance problem. By utilizing the joint space domain, the error term defined has combined the two errors by avoiding the issue of mixed dimensions or non-homogeneous terms. The work presented sets up a scheme that could be used to apply optimization techniques in the design of other closed loop mechanisms.

This method is computationally intensive due to the iterative nature of the algorithm. The method was implemented using Matlab 7.0 software on a Intel Core2 T5300 (1.73Ghz) processor, with a 2 Gb ram. With parallel processing disabled, a single run for the code took about 996.32 CPU seconds to calculate the error for the example listed previously. However, since each path is independent of the other, this method is suited for parallel architecture and parallel processing will greatly improve the speed.

The geometry of having consecutive axes parallel greatly increases the simplicity of the gears that are used to couple the joint axes. The problem can be broadened where the mechanism geometry is changed to simplify the inverse analysis problem and non-planar non-circular gears are used to couple consecutive axes. The error functional in such a case would be the same as the one presented in this paper. The problem of extending this method to mechanisms with a different geometry is being investigated.

REFERENCES


[1] M. Bodduluri, J. Ge, M. J. McCarthy, B. Roth, The Synthesis of Spatial Linkages, Modern Kinematics: Developments in the Last Forty Years, J. Wiley and Sons, New York, 1993.

[2] B. Roth, Analytic design of open chains, in: O. Faugeras, G. Giralt (Eds.), Third International Symposium of Robotic Research, MIT Press, 1986.

[3] L. W. Tsai, Design of open loop chains for rigid body guidance, Ph.D. thesis, Stanford University (1972).

[4] C. H. Suh, C. W. Radcliffe, Kinematics and Mechanism Design, Wiley and Sons, New York, New York, 1978.

[5] E. Lee, C. Mavroidis, J. P. Merlet, Five precision point synthesis of spatial rrr manipulators using interval analysis, Journal of Mechanical Design 126 (5) (2004) 842–849.

[6] A. P. Morgan, C. W. Wampler, Solving a planar four-bar design problem using continuation, Journal of Mechanical Design 112 (4) (1990) 544–550.

[7] C. W. Wampler, A. P. Morgan, A. J. Sommese, Numerical continuation methods for solving polynomial systems arising in kinematics, Journal of Mechanical Design 112 (1) (1990) 59–68.

[8] B. Roth, F. Freudenstein, Synthesis of path generating mechanisms, Journal of Engineering for Industry 85B (1963) 298–306.

[9] C. W. Wampler, A. P. Morgan, A. J. Sommese, Complete solution of the nine-point path synthesis problem for four-bar linkages, Journal of Mechanical Design 114 (1) (1992) 153–159.

[10] V. I. Kulyugin, Design of three dimensional four-link mechanisms conforming to the travel of the driven link and coefficient of increase in velocity of the reverse stroke, in: Analysis and Synthesis of Mechanisms, Amerind Publishing Co. Pvt. Ltd., 1975, pp. 152–162.

[11] J. K. Salisbury, J. J. Craig, Articulated hands: Force control and kinematic issues, The International Journal of Robotics Research 1 (1) (1982) 4–17.

[12] L.-W. Tsai, S. Joshi, Kinematics and optimization of a spatial 3-upu parallel manipulator, Journal of Mechanical Design 122 (4) (2000) 439–446.

[13] J. R. Mckinley, C. Crane, D. Dooner, Reverse kinematic analysis of the spatial six axis robotic manipulator with consecutive joint axes parallel, in: International Design Engineering Technical Conferences & Computers and Information in Engineering Conference, no. DETC2007-34433, ASME, Las Vegas, 2007.

[14] J. R. Mckinley, Three-dimensional rigid body guidance using gear connections in a robotic manipulator with parallel consecutive axes, Ph.D. thesis, University of Florida (2007).

[15] V. Krovi, G. K. Ananthasuresh, V. Kumar, Kinematic and kinetostatic synthesis of planar coupled serial chain mechanisms, Journal of Mechanical Design 124 (2) (2002) 301–312.

[16] Y.-W. Pang, V. Krovi, Kinematic synthesis of coupled serial chain mechanisms for planar path following tasks using fourier methods, in: ASME Design Engineering Technical Conferences, no. DETC2000/MECH-14188, ASME, Baltimore, Maryland, 2000.

[17] R. S. Ball, A Treatise on the Theory of Screws, University Press, Cambridge, 1900.

[18] K. H. Hunt, Kinematic Geometry of Mechanisms, Clarendon Press; Oxford University Press, Oxford; New York, 1978.

[19] J. Duffy, C. Crane, A displacement analysis of the general spatial 7-link, 7r mechanism, Mechanism and Machine Theory 15 (3) (1980) 153 – 169.

[20] H.-Y. Lee, C.-G. Liang, Displacement analysis of the general spatial 7-link 7r mechanism, Mechanism and Machine Theory 23 (3) (1988) 219 – 226.

[21] J. M. Rico, J. Gallardo, J. Duffy, Screw theory and higher order kinematic analysis of open serial and closed chains, Mechanism and Machine Theory 34 (4) (1999) 559 – 586.

# BIOGRAPHICAL SKETCH

Mandar Harshe was born in 1985 in Mumbai, India. He did his schooling in E.N.N.S School, Pune and attended junior college at Fergusson College, Pune. He then attended M.E.S College of Engineering, affiliated with the University of Pune, and graduated with a Bachelor of Engineering in mechanical engineering in June 2007. He did his degree project at Nirmiti Stampings Pvt Ltd, Pune, India where he worked on developing a low cost robotic arm. In August 2007, he joined the Center for Intelligent Machines and Robotics (CIMAR) at the University of Florida, and received his Master of Science degree in the spring of 2009. He plans to pursue to his doctorate in the area of mechanism theory focusing on kinematics and computational geometry.